

## *Cryptococcus neoformans* Gene Expression during Experimental Cryptococcal Meningitis

B. R. Steen,<sup>1</sup> S. Zuyderduyn,<sup>2</sup> D. L. Toffaletti,<sup>3</sup> M. Marra,<sup>2</sup> S. J. M. Jones,<sup>2</sup>  
J. R. Perfect,<sup>3</sup> and J. Kronstad<sup>1\*</sup>

Biotechnology Laboratory, Department of Microbiology and Immunology, and Faculty of Agricultural Sciences, The University of British Columbia, Vancouver, British Columbia V6T 1Z3,<sup>1</sup> and Genome Sciences Centre, British Columbia Cancer Agency, Vancouver, British Columbia V5Z 4E6,<sup>2</sup> Canada, and Department of Medicine, Duke University Medical Center, Durham, North Carolina 27710<sup>3</sup>

Received 9 August 2003/Accepted 22 September 2003

***Cryptococcus neoformans*, an encapsulated basidiomycete fungus of medical importance, is capable of crossing the blood-brain barrier and causing meningitis in both immunocompetent and immunocompromised individuals. To gain insight into the adaptation of the fungus to the host central nervous system (CNS), serial analysis of gene expression (SAGE) was used to characterize the gene expression profile of *C. neoformans* cells recovered from the CNS of infected rabbits. A SAGE library was constructed, and 49,048 tags were sequenced; 16,207 of these tags were found to represent unique sequences or tag families. Of the 304 most-abundant tags, 164 were assigned to a putative gene for subsequent functional grouping. The results (as determined according to the number of tags that identified genes encoding proteins required for these functions) indicated that the *C. neoformans* cells were actively engaged in protein synthesis, protein degradation, stress response, small-molecule transport, and signaling. In addition, a high level of energy requirement of the fungal cells was suggested by a large number of tags that matched putative genes for energy production. Taken together, these findings provide the first insight into the transcriptional adaptation of *C. neoformans* to the host environment and identify the set of fungal genes most highly expressed during cerebrospinal fluid infection.**

*Cryptococcus neoformans* is an opportunistic pathogen that primarily infects immunocompromised individuals. Infection is generally initiated by inhalation of basidiospores or poorly encapsulated yeast cells and is usually contained by granulomatous inflammation within the lung in immunocompetent individuals. In immunocompromised hosts, the fungus is frequently capable of disseminating into the bloodstream and then crossing the blood-brain barrier to cause meningoencephalitis (52). *C. neoformans* has emerged as a significant opportunistic pathogen because of the pandemic of AIDS and the widespread use of immunosuppressive therapy; this fungus now represents the most common cause of fungal infections of the central nervous system (CNS) (68). CNS cryptococcosis is fatal without treatment, and therapy with the antifungal drug amphotericin B has limitations due to potential host toxicity. Treatment failures with death in the first 3 months after diagnosis still range between 10 and 25%. The importance of identifying new targets for antifungal therapy is emphasized by a recent outbreak of *C. neoformans* infections on Vancouver Island in British Columbia, Canada. None of the approximately 60 cases involved people coinfecting with human immunodeficiency virus, and the disease occurred primarily in immunocompetent individuals (84).

The best-characterized virulence factors for *C. neoformans* include the production of a polysaccharide capsule, the formation of melanin, and the ability to grow at 37°C (71). Capsule-

defective mutants of *C. neoformans* and mutants defective in their ability to grow at 37°C are essentially avirulent; mutants defective in melanin production display attenuated virulence (19, 50, 63, 65, 96). The capsular polysaccharide is believed to be antiphagocytic, because phagocytes do not ingest the fungal cells in vitro in the absence of complement or antibodies (47, 48) and the capsule blocks the recruitment of inflammatory cells (reviewed by Rodrigues et al. [76]). Capsular polysaccharide also depletes complement and suppresses the delayed type of hypersensitivity response and may influence antibody production during fungal infection. In vitro studies have shown that compared with nonencapsulated cells, encapsulated cells are better able to resist phagocytosis. Recent in vivo studies indicate that *C. neoformans* is actually a facultative intracellular pathogen and that polysaccharide production within phagocytic cells contributes to fungal survival (reviewed by Feldmesser et al. [30]).

Melanin formation in *C. neoformans* is catalyzed by a laccase that uses diphenolic compounds such as catecholamines as substrates (77). Melanin is synthesized during infection and is hypothesized to serve a protective function by quenching free radicals (63, 95). The prevalence of substrates for laccase in the CNS has been proposed as a possible explanation for the neurotropism of the fungus (17, 62).

The mechanisms of thermotolerance in *C. neoformans* are starting to be explored. Genes such as *RASI* (encoding a small GTP-binding protein) and *CNA1* (encoding calcineurin) have been implicated during growth at elevated temperatures (3, 65). Steen et al. have recently initiated a genome-wide analysis of the response of *C. neoformans* to host temperature (83). This analysis revealed striking differences in the levels of re-

\* Corresponding author. Mailing address: Biotechnology Laboratory, University of British Columbia, 237-6174 University Blvd., Vancouver, B.C. V6T 1Z3, Canada. Phone: 604-822-4732. Fax: 604-822-2114. E-mail: kronstad@interchange.ubc.ca.

sponsiveness of serotype A and D strains to growth at 25 versus 37°C. Our analysis of the response to the temperature difference in a serotype D strain revealed changes in transcript levels for histone genes, stress-related genes, and genes encoding translation components.

We are interested in identifying the factors that are important for *C. neoformans* to survive and proliferate in the cerebrospinal fluid (CSF) of an infected host. The rabbit is an excellent model for cryptococcal meningitis because it allows study of the yeast at the site of infection in a serial manner, and this is difficult to perform in smaller animals such as mice, rats, or guinea pigs (23). The body temperature of the rabbit (39.5°C) and the use of steroids in this model are meant to closely mimic the human host situation in which patients usually present with fever and are often undergoing steroid treatment (68). We applied the technique of serial analysis of gene expression (SAGE) to *C. neoformans* cells isolated from the CSF of rabbits to characterize the transcript abundance profile under these specific *in vivo* conditions.

SAGE was chosen instead of microarray analysis due to the limited number of expressed sequence tags (ESTs) and the availability of the genomic sequence of *C. neoformans* strain H99 at the start of our work. SAGE involves the construction and sequencing of libraries of short (10- to 14-bp) sequence tags in which each tag represents a single unique transcript in the cell. The number of times a unique tag sequence appears in a library of SAGE tags is directly proportional to and accurately represents the RNA expression level of the corresponding gene under the specified growth conditions (91). Recent studies indicate that the microSAGE and the SAGE methods are reproducible and accurate for libraries made separately from the same starting material (13, 88).

Our preliminary analysis of the 304 most highly expressed SAGE tags from *C. neoformans* cells isolated from the rabbit CSF revealed several categories of gene functions, including protein biosynthesis and degradation, energy production, stress response, signaling, and small-molecule transport as well as carbohydrate, amino acid, and lipid metabolism. The high level of expression of genes in these categories suggested that these are functions that *C. neoformans* requires to survive and proliferate within the host environment. These findings will be important for the *C. neoformans* research community, and further functional analysis of the genes that we have identified may shed light on the propensity of *C. neoformans* to cause life-threatening meningitis. In addition, our SAGE data are valuable for the annotation of the H99 genome because they identify transcribed regions.

#### MATERIALS AND METHODS

**Strains and growth conditions.** The *C. neoformans* serotype A, *MAT $\alpha$*  strain H99 was used for the rabbit infection. The growth conditions for the *in vitro* 25°C and 37°C SAGE libraries have been described previously (83). Briefly, cells were cultured overnight with shaking in yeast nitrogen base (YNB) broth at either 25°C or 37°C until the cells reached log phase. Cells were harvested by centrifugation, snap frozen, and then lyophilized.

**Rabbit cryptococcal meningitis model.** New Zealand White rabbits were housed in separate cages and provided with water and Purina rabbit chow ad libitum. Each rabbit weighed between 2 and 3 kg. H99 cells were grown for 3 to 4 days on YPD plates and then transferred to YNB broth supplemented with 2% glucose (with shaking at 30°C for 48 h). The cells were pelleted and washed once in phosphate-buffered saline and then suspended in phosphate-buffered saline at a concentration of  $3.25 \times 10^9$  cells per ml. New Zealand White rabbits were

immunosuppressed with betamethasone acetate-phosphate (Schering-Plough, Kenilworth, N.J.) 24 h prior to inoculation with H99 and then daily throughout the infection. After sedation with ketamine (Fort Dodge Laboratories, Fort Dodge, Iowa) and xylazine (Vedco, St. Joseph, Mo.),  $1.3 \times 10^9$  viable *C. neoformans* cells in a volume of 0.4 ml were inoculated intracisternally into each of 12 rabbits. The rabbits were sedated on days 5, 7, and 9 after inoculation, and the CSF (0.3 to 0.7 ml) was withdrawn from the subarachnoid space, pooled, and immediately placed on ice until RNA processing was performed. Cryptococci in the pooled CSF samples were counted, with the following results: on day 5,  $5.2 \times 10^7$  yeast cells were found; on day 7,  $2.2 \times 10^7$  yeast cells were found, and on day 9,  $4.0 \times 10^6$  yeast cells were found. Samples were split into two aliquots, pelleted at 4°C, washed in chilled water, and allowed to sit on ice for 5 to 10 min to lyse any rabbit cells that may have been present. The supernatant was then withdrawn, and the pellet was frozen at -80°C for lyophilization.

**RNA isolation.** One-half of the lyophilized cells from days 5, 7, and 9 of infection were pooled and vortexed with 1.0-mm-diameter acid-washed, RNase-free silica matrix beads for 15 min. Beads and yeast cells were resuspended in 1.0 ml of TRIzol (Gibco BRL) and incubated at room temperature for 15 min. Total RNA was isolated according to the instructions of the manufacturer (Gibco BRL), and the pellet was dissolved in 1.0 ml of lysis-binding buffer from a Dynabeads mRNA DIRECT kit (Dyna). Beads were prepared per the instructions of the manufacturer (Dyna), and mRNA was added to the beads. Poly(A)<sup>+</sup> RNA was isolated per the microSAGE method (detailed protocol version 1.0e; available at [www.sagenet.org](http://www.sagenet.org)).

**SAGE analysis.** The microSAGE method was performed per the microSAGE protocol. A total of 35 PCR cycles were performed to amplify the ditags during the construction of the library. The library of clones was sequenced by BigDye primer cycle sequencing on an ABI PRISM 3700 DNA analyzer. Sequence chromatograms were processed using PHRED software (28, 29), and the vector sequence was detected and removed using CROSS\_MATCH software (36). Tags (10 bp) (plus the 4-bp *Nla*III site) were extracted, and each tag was given a quality (accuracy) score based on the cumulative PHRED score. Only tags with an accuracy of more than 99% were used in this study. *P* values for comparisons of levels of tag abundance between libraries were determined and represented the probability that the difference in tag numbers was due to random fluctuation (10).

**Tag identification.** For preliminary assignment of tags to putative genes, we used the EST database available for strain H99 at the University of Oklahoma's Advanced Center for Genome Technology (<http://www.genome.ou.edu/cneo.html> [funded under cooperative agreement UO1 AI 485 94-01]). When an EST sequence could not be identified for a particular tag, we used the genomic sequence available for H99 at the Duke University Center for Genome Technology (<http://cgt.genetics.duke.edu/data/index.html>) and the Whitehead Institute Center for Genomic Research ([http://www-genome.wi.mit.edu/annotation/fungi/cryptococcus\\_neoformans/index.html](http://www-genome.wi.mit.edu/annotation/fungi/cryptococcus_neoformans/index.html)) to identify contigs with unambiguous tag assignments. Once an EST or genomic sequence had been identified, the BLASTx (Basic Local Alignment Search Tool) algorithm was employed to find proteins of high levels of sequence similarity in the nonredundant database at the National Center for Biotechnology Information (NCBI). Each BLASTx result was inspected individually and recorded. In the case of genomic DNA sequences where introns are present, the expected values recorded were higher than would have been expected if the introns had been removed. The same was true for the results determined for both genomic DNA sequences and ESTs compared to those that would have been expected if the sequences had been translated and the BLASTp algorithm were employed rather than a BLASTx algorithm.

#### RESULTS AND DISCUSSION

**Overview of highly expressed SAGE tags *in vivo*.** *C. neoformans* H99 cells were pooled from the CSF of 12 rabbits on days 5, 7, and 9 postinfection, and the microSAGE method was used to generate a library of cDNA tags. The microSAGE method was used rather than the standard protocol due to the small number of cells obtained from infected animals ( $8.3 \times 10^7$  cells) and the difficulty of obtaining large amounts of RNA from *C. neoformans* due to its large polysaccharide capsule. The microSAGE library was sequenced to generate *C. neoformans* gene expression data. The total number of tags for this library was 49,048, and 16,207 of these tag sequences were unique in the library, 10,305 tags occurred once, and 5,902 tags

TABLE 1. Abundance classes

Interval	Tag sequence count	Total no. of tags
1	10,305	10,305
2-4	4,183	10,426
5-9	1,007	6,436
10-99	685	16,651
100-99	27	5,230
Total	16,207	49,048

occurred more than once. These numbers provide an approximation of the total number of genes expressed under these growth conditions, although it is difficult to estimate gene numbers from SAGE data (85).

An overview of the abundance classes for the in vivo library is presented in Table 1. Both the number of different tag sequences and the total number of tags present in each abundance class are indicated. For example, in the largest abundance class, 685 SAGE tag sequences appear between 10 and 99 times for a total of 16,651 tags. The in vivo library tag distribution is slightly different from that of the abundance classes for the temperature SAGE libraries that were previously characterized (83). Figure 1 presents the distribution of the tags in abundance classes for the in vivo library, as well as those of the 25 and 37°C in vitro libraries for comparison. To do the direct comparisons, the libraries were normalized to the size of the smallest library and tags that appeared less than one time in any given library were removed. The most striking difference occurs upon comparison of the in vivo data with that of the 37°C in vitro library; by contrast, the in vivo library appears to be more similar to the 25°C in vitro library in terms of overall tag abundance.

To study further the relationship between in vivo and in vitro growth, a global comparison of the numbers of shared tags among the three libraries was performed to generate an overview of the SAGE data (Fig. 2). The Venn diagram shows that the in vivo library shared 1,885 SAGE tag sequences with the 25°C library alone and 632 SAGE tag sequences with the 37°C library alone. Of the remaining in vivo tags, 12,231 were unique to the in vivo library and 1,459 were shared by all three libraries. As well, this analysis revealed that the 25°C in vitro library was 92.3% similar to the in vivo library in terms of overall gene expression patterns relative to an 88.1% similarity between the 37°C library and the in vivo library. Importantly, we have found that a large proportion of the most highly expressed genes in vivo (described below) were also found among the most highly expressed genes in vitro at 25°C (B. Steen, unpublished observations). Specifically, 69% of those tags that are more abundant at 25 than at 37°C are also found in the most abundant tags of the in vivo library. This suggests that much of the similarity between the in vivo and the 25°C libraries is represented in the most abundant tags (83). Taken together, these data support the hypothesis that the *C. neoformans* transcription profile from cells grown in vivo is more similar to that of cells grown in vitro at 25°C than to that of those grown at 37°C.

To gain an understanding of the predisposition of *C. neoformans* for the CNS, we attempted to determine which genes were highly expressed during CNS infection by strain H99. To

do so, we chose the 304 most-abundant tags and used those to predict genes from the EST and genomic sequences of strain H99. We then determined what the abundance of these same tags was in the in vitro temperature libraries.

An assembly of shotgun sequence data recently became available for the genome of *C. neoformans* strain H99 (18 February 2003, 2× coverage, Duke Center for Genome Technology; 13 June 2003, 11× coverage, Whitehead Institute Center for Genome Research). Combined with an EST database (*Cryptococcus neoformans* cDNA Sequencing Project, University of Oklahoma), these resources allowed us to give preliminary gene assignments to 164 of the top 304 most-abundant SAGE tags in the *C. neoformans* in vivo library. The remaining 140 tags yielded four types of results in BLAST searches. First, 31 (10%) of the top 304 SAGE tags did not hit any of the sequences in either the H99 genomic or EST databases. These tags were then used in a BLAST search of the available *Oryctolagus cuniculus* (rabbit) EST sequences at NCBI and of the genomic sequence (sequenced by the National Cancer Institute; available at the ENSEMBLE trace server). We were able to confirm that these tags were not a result of the presence of contaminating cells from the rabbit CSF. Second, 85 (28%) of the SAGE tags corresponding to ESTs or genomic contigs did not result in significant BLAST scores in searches of the non-redundant database at NCBI. Third, 13 (4%) of the tags were significantly similar to uncharacterized, hypothetical proteins. Finally, 11 (3.6%) of the tags hit more than one EST or genomic contig such that further characterization was not possible.

Table 2 shows the 164 tags that were given putative gene identifications; these results were then classified according to the controlled vocabulary determined by the Gene Ontology (GO) Consortium (9). Normalization of the data to the size of the smallest library (the 25°C in vitro library) allowed a comparison of tag abundance in vivo to the abundance of the same tags in vitro at either 25 or 37°C. It should be noted, however, that this comparison involved libraries prepared from cells grown under different conditions of temperature (e.g., 39.5°C in the rabbit) and nutrition (i.e., YNB broth for the in vitro libraries).

**Protein biosynthesis.** Of the 164 annotated SAGE tags, 46 were assigned to ribosomal protein genes and 5 more were assigned to genes for two translation elongation factors, two translation initiation factors, and a poly(A)-binding protein. The expectation of this abundance of transcripts encoding translation factors was determined on the basis of SAGE experiments for *Saccharomyces cerevisiae* grown in rich medium in vitro at 30°C. For example, SAGE analysis of *S. cerevisiae* revealed that mRNAs for ribosomal proteins represented 18 of the 30 most abundant transcripts (92). Our results indicated that the *C. neoformans* cells were proliferating in the CSF of rabbits and carrying out protein biosynthesis. Little is known about the regulation of protein biosynthesis in *C. neoformans*. The results of several studies with *S. cerevisiae* indicate that ribosome production is a major consumer of cellular resources and is a key component of the energy budget of the cell. Several factors regulate the production of ribosomal proteins in yeast, including nutrients such as nitrogen via the TOR signaling pathway (16, 79) and carbon source through the cyclic AMP (cAMP)/protein kinase A (PKA) signaling pathway (46).

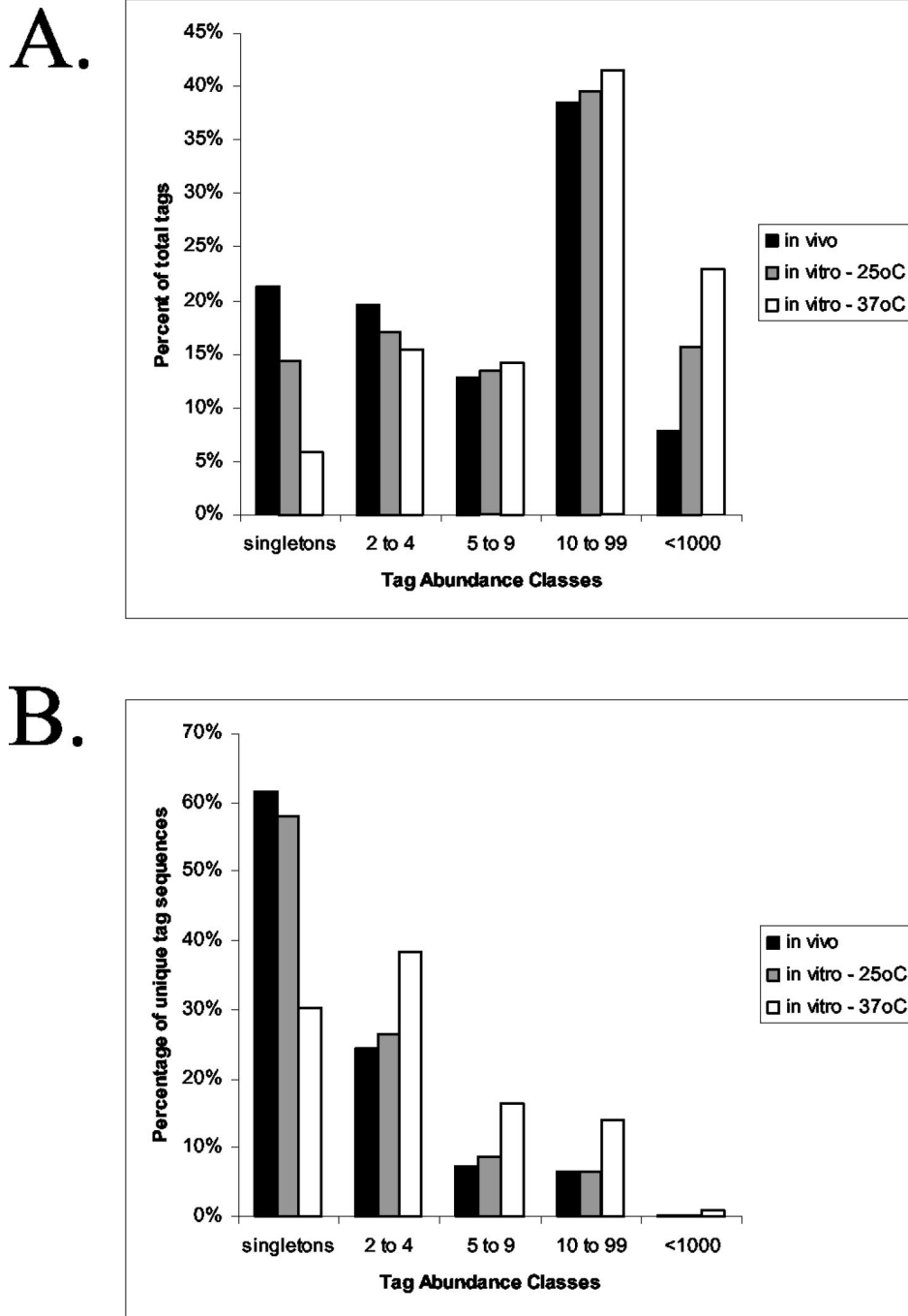


FIG. 1. Tag distribution in three SAGE libraries. Tags were grouped into categories to illustrate their distribution for the SAGE library constructed from *C. neoformans* cells grown in the cerebral spinal fluid of rabbits relative to those for the in vitro 25°C and 37°C libraries. The percentage of the total tags that were found in each abundance class is shown (A), and the percentage of unique tag sequences for each abundance class is also presented (B).

Additionally, the interruption of secretory pathway signals (mediated by protein kinase C) results in the repression of ribosomal protein biosynthesis (53). Finally, it is known that the levels of ribosomal protein mRNAs are significantly higher in rapidly growing cells than in cells that are growing more slowly (99).

Interestingly, upon comparison of the abundance of the 51

translation-related tags with results from in vitro temperature libraries, we found that 37 (73%) were most abundant in vivo relative to the in vitro situation. Six of the remaining ribosomal protein tags (*RPS12*, *RPL1*, *RPL30*, *RPL36A*, *RPL37B*, and *RPL41* plus *TEF1*) were most abundant at 37°C relative to both the 25°C library and the in vivo library. *RPL18* and *RPS26* were most abundant at 25°C, and the remaining tags were



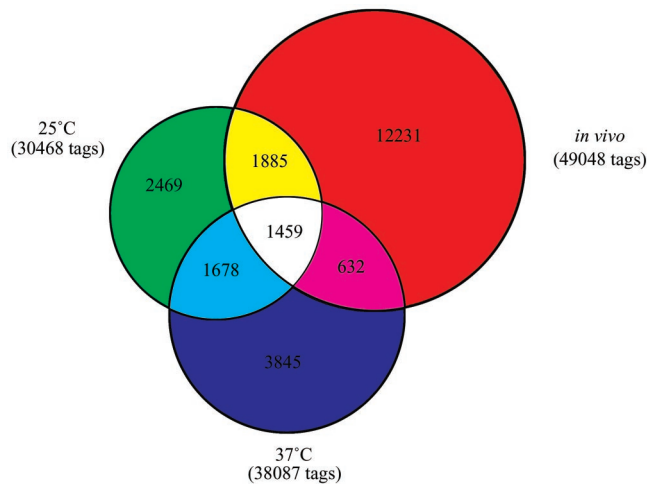


FIG. 2. Shared SAGE tags among the three libraries. The Venn diagram shows the number of tags that were unique to each library such that the overlapping regions illustrate the number of tags shared by each of two libraries and the number of tags found in all three libraries.

equally abundant both at 25°C and in vivo. It is interesting that all six of the ribosomal protein transcripts and *TEF1* (which are more abundant at 37°C than in vivo) exhibit a significantly higher abundance overall than all of the other ribosomal protein transcripts at the same temperature. This suggests that not all ribosomal protein genes are transcribed equally at 37°C and that novel regulatory functions influence the transcription of these seven genes.

A tag for the phosphomannomutase gene was highly abundant under in vivo conditions relative to in vitro conditions. In *S. cerevisiae*, this enzyme is known to be required for O-linked glycosylation of proteins and is involved in protein secretion. A phosphomannomutase mutant in yeast displays defective ribosomal protein synthesis due to the strong regulatory link between protein biosynthesis and secretion pathways (60). Our findings here suggest that the protein biosynthesis and secretory pathways are also tightly linked in *C. neoformans*.

**Protein catabolism.** In addition to the evidence for active protein biosynthesis in vivo, several tags identified genes encoding proteins required for protein degradation. For example, the presence of abundant tags for ubiquitin pathway genes suggests proteasome activity in the *C. neoformans* cells in the host environment. Ubiquitin is transferred to proteins that are targeted for degradation by ubiquitin-conjugating or -ligating enzymes (identified by our SAGE tags), and proteasome activity is involved in several cell processes, including regulation of the cell cycle, transcription, signal transduction, and apoptosis (reviewed in reference 37). We also identified a SAGE tag corresponding to ubiquitin/S27a fusion protein; ubiquitin serves to aid in the assembly of S27a into the ribosome, and this result suggests a possible connection with the translation machinery (31).

In the context of proteolysis, we also identified tags for four proteases that were abundant in vivo. The two metalloproteases that we identified were not abundant in vitro regardless of temperature. The carboxypeptidase tag was abundant in

vitro, but to a lesser extent relative to the abundance seen under in vivo conditions, and the proteinase A gene was temperature regulated and abundant both in vivo and at 25°C in vitro. These proteases may be important virulence factors because of their potential involvement in the degradation of host tissues and the proteolysis of immunologically important host proteins such as antibodies and complement. It is known that *C. neoformans* produces many extracellular enzymes that may contribute to its ability to invade host tissues (21, 22, 76). In the context of in vivo growth, the CSF contains some plasma-derived proteins, including low concentrations of immunoglobulins and C'3 complement. However, the concentration of these and other proteins in the CSF is significantly less than the concentration of the same proteins in the plasma, such that the CSF is regarded as protein poor (24). Therefore, *C. neoformans* may secrete proteases for the assimilation of carbon and nitrogen to enable growth in the relatively nutrient-deficient CSF. There is evidence to support the supposition that *C. neoformans* secretes proteases to use proteins as a nitrogen source (8). In addition, we identified tags for glutamine synthetase and glutamine-dependent NAD<sup>+</sup> synthase (both categorized under the GO heading amino acid metabolism; see Table 2). Glutamine synthetase exhibits increased activity under conditions of nitrogen starvation in *Candida albicans* (38). Glutamine-dependent NAD<sup>+</sup> synthase is responsible for the use of glutamine as an ammonia source (98). As determined on the basis of tag abundance, our findings support the hypothesis that protease production is an important requirement for survival of *C. neoformans* in the CSF.

**Response to stress.** Several tags corresponded to genes known to be involved in protein folding and the response to heat stress (Table 2). Heat shock proteins are produced in cells under conditions of stress and allow cells to survive under conditions that would otherwise be lethal (35, 66). They play a role in the folding and unfolding of proteins, the degradation of unstable proteins, the prevention of protein aggregation, and the transport of proteins within the cell. Interestingly, the two most-abundant tags overall corresponded to two different putative heat shock protein 12 genes (*HSP12*) and both were more abundant in strain H99 at 25 than at 37°C. This is similar to what was observed in the SAGE temperature libraries for one of the *HSP12* genes in the serotype D strain B3501 (83). Although a second *HSP12* has also been identified in the genomic DNA sequence of strain B3501, no SAGE tag was identified in the serotype D in vitro temperature data. A SAGE tag for heat shock protein 60 (Hsp60p) was also identified; this protein is known to produce a strong immune response in the host during infection with *Coccidioides immitis* (87) and *Histoplasma capsulatum* (78). Studies of *H. capsulatum* demonstrate the use of Hsp60p and fragments of this protein as an effective vaccine (25). In addition, the identification of *HSP90* in our SAGE data is interesting, because the *C. albicans* Hsp90p is immunogenic and can confer protective immunity in a mouse model (58). *HSP70* was also identified as highly abundant in vivo and is known to be a major immunogenic antigen during pulmonary cryptococcosis (42, 43). Taken together, these studies with Hsp60p, Hsp70p, and Hsp90p in other fungi and our SAGE data suggest that all of these proteins can thus serve as good vaccine candidates for patients at risk for cryptococcal meningitis.

TABLE 2. Annotated SAGE tags found in the top 304 most-abundant tags expressed in vivo<sup>a</sup>

Function and tag	No. of tags detected			BLAST result	Species	E value	% Identity	% Similarity
	In vivo	25°C	37°C					
<b>Protein biosynthesis</b>								
CGACAGACCG	195 <sup>a</sup>	235	1160	Translation elongation factor 1 (TEF1)	Annotated			
AGTACTCTTC	174	11	11	Ribosomal protein P2	<i>Podospira anserina</i>	1.0E-26	57	65
GCATTCTTTA	172	15	4	40S ribosomal protein s11	<i>Schizosaccharomyces pombe</i>	8.0E-54	72	80
TATGATAGTG	143	34	0	60S ribosomal protein L7a (L8)	<i>S. pombe</i>	3.0E-82	66	79
GCAGATCTAT	134	31	27	Ribosomal protein RPL39	Annotated			
GATGCTCTGT	43	10	0	Ribosomal protein RPL39	Annotated			
TCGTCTGAAG	101	31	19	60S ribosomal protein L5B	<i>S. pombe</i>	3.0E-98	61-66 (2) <sup>b</sup>	78
AGAACTCAA	91	2	3	40S ribosomal protein S6B	<i>S. pombe</i>	4.0E-75	65	74
ACTACGTTCT	86	39	17	60S acidic ribosomal protein p1	<i>S. pombe</i>	6.0E-22	48	61
TATACCTATG	89	29	2	40S ribosomal protein s3ae (S1)	<i>S. pombe</i>	2.0E-85	68	81
AACCTTGCAT	88	21	5	Ribosomal protein L20A	<i>S. pombe</i>	2.0E-47	56-68 (3)	65-78 (3)
GGTTTGTACA	82	13	7	Probable ribosomal protein S29	<i>Neurospora crassa</i>	3.0E-05	77-83	81-100
ACATTTCCGA	81	32	7	Putative ribosomal protein L14B	<i>Takifugu rubripes</i>	1.0E-25	52	69
ACATCGATCT	81	38	4	60S ribosomal protein L31	<i>Nicotiana glutinosa</i>	8.0E-25	49-70 (2)	65-87 (2)
CACATTGATA	75	7	4	Ribosomal protein L13A	<i>Xanthophyllomyces dendrorhous</i>	2.0E-80	72	81
CATTGTGACT	74	27	5	Ribosomal protein S7	<i>Xenopus laevis</i>	4.0E-40	52	68
TATTCATAAC	72	7	2	60S ribosomal protein L37A	<i>Saccharomyces cerevisiae</i>	9.0E-34	79	87
CACTTCGATC	67	29	9	60S ribosomal protein L23	<i>S. pombe</i>	3.0E-61	80	93
TAACCCAAAT	65	16	5	60S ribosomal protein L7	<i>Caenorhabditis elegans</i>	3.0E-66	50	66
TTACACAGCA	64	8	27	Putative ribosomal protein S19	<i>Pleurotus ostreatus</i>	3.0E-41	77	84
AACGGTTATG	62	34	6	Ribosomal protein L3	<i>Spodoptera frugiperda</i>	1.0E-44	65	75
CATTGAGGTT	62	31	18	Ribosomal protein S22	<i>Candida albicans</i>	2.0E-31	56	64
GCTTCACAGA	59	21	2	60S ribosomal protein L12	<i>Mus musculus</i>	6.0E-61	70	81
ACTATCACAA	59	10	4	60S ribosomal protein L27A	<i>S. pombe</i>	1.0E-49	66	84
GTCTCTTTAC	58	12	6	60S ribosomal protein L10A	<i>S. pombe</i>	8.0E-75	63	77
CACGGCGCAT	56	3	185	Ribosomal protein L41	Annotated			
TATTACAGCT	55	5	1	60S ribosomal protein L6	<i>Arabidopsis thaliana</i>	5.0E-08	41	60
TGGATGAGAT	53	9	33	40S ribosomal protein S3	<i>N. crassa</i>	2.0E-92	79	87
CATCTTTCCT	52	25	4	Ribosomal protein P0	<i>P. anserina</i>	2.0E-86	59	74
GAGTTGTTGA	50	41	123	60S ribosomal protein L36A	<i>S. pombe</i>	5.0E-65	61	77
CTTTGGATCA	48	3	2	60S ribosomal protein L30/L30A	<i>S. pombe</i>	4.0E-23	79	92
TAAATGGTGC	47	11	0	Ribosomal protein RPL22	Annotated			
ATCCCGTGGC	46	38	8	40S ribosomal protein S14	<i>Podocoryne carnea</i>	4.0E-41	66	72
GGCCGACCTG	45	85	286	Ribosomal protein L1	<i>S. pombe</i>	5.0E-56	52-58 (2)	61-64 (2)
AAGGGTGGTG	43	69	229	Ribosomal protein L24A (L30)	<i>Kluyveromyces lactis</i>	2.0E-34	54	67
AGAGATTCT	43	7	3	Translation elongation factor 2 (TEF2)	Annotated			
TATGATTTTA	43	8	7	40S ribosomal protein S28	<i>N. crassa</i>	1.0E-59	80	85
AAGGACTCTC	43	50	181	Cytoplasmic ribosomal protein S12	<i>P. anserina</i>	4.0E-43	60	67
TACGATTGCG	40	28	5	Translation initiation factor eIF-5A	<i>C. albicans</i>	1.0E-62	81	91
ACAAAAAAA	39	7	3	Ribosomal protein L35	<i>Paracoccidioides brasiliensis</i>	3.0E-29	57	69
GATGCTTTTT	38	24	1	60S ribosomal protein L19B	<i>S. pombe</i>	2.0E-54	55	68
CTATTGGTCG	33	4	6	40S ribosomal protein S8	<i>Schizophyllum commune</i>	2.0E-29	83	87
CAACGGGGGG	29	7	0	Phosphomannomutase	<i>C. albicans</i>	2.0E-09	56	80
CACCACATTC	26	37	7	60S ribosomal protein L18	<i>S. pombe</i>	1.0E-58	65	74
ATATTCTAT	25	1	0	Eukaryotic translation initiation factor 4A2	<i>M. musculus</i>	7.0E-23	77	90
ACTGGATGAG	24	19	18	Poly(A) binding protein RB47	<i>Chlamydomonas reinhardtii</i>	7.0E-28	46	53
CTCTCTATGT	23	3	3	40S ribosomal protein S24	<i>N. crassa</i>	4.0E-21	48	60
AAGCGATTTT	22	71	19	40S ribosomal protein S26	<i>S. commune</i>	5.0E-20	56-79 (3)	66-97 (3)
CTCTTCCCT	21	33	145	Ribosomal protein L37B	<i>S. cerevisiae</i>	4.0E-32	59	81
GCTTCCACGA	21	4	0	Ribosomal protein L23A	<i>Puccinia graminis</i>	1.0E-41	71	81
<b>Protein catabolism</b>								
CACATTCTTT	81	19	8	Ubiquitin/S27a fusion protein [imported]	<i>N. crassa</i>	2.0E-39	53	66
ACTATCGCCT	58	21	4	Ubiquitin conjugating enzyme UBC1	<i>Glomerella cingulata</i>	6.0E-35	73	79
TGTATGGTCT	40	6	5	Metalloprotease	<i>Aspergillus fumigatus</i>	5.0E-27	39	52
GATCCAATAT	39	42	4	Proteinase A	<i>Pichia angusta</i>	7.0E-36	49	63
ATGAAAAAAA	38	52	1	Ubiquitin transferase	<i>S. pombe</i>	4.0E-08	57	67
TCTCTCCGT	30	16	10	Carboxypeptidase	<i>Penicillium janthinellum</i>	1.0E-35	69	77
GCTGGAGAGA	30	6	0	Zinc metalloprotease	<i>N. crassa</i>	2.0E-35	46	58
AACTTCATTG	14	6	0	Metacaspase	<i>Aspergillus nidulans</i>	8.0E-80	26-64 (4)	36-79 (4)
<b>Response to stress</b>								
TATATGTGTA	637	31	0	Heat shock protein 12	<i>S. cerevisiae</i>	1.0E-06	45	61
TGACTGTTTA	468	57	4	Heat shock protein 12	<i>Saccharomyces pastorianus</i>	9.0E-04	5	73
TATATATGCA	107	3	2	Heat shock protein 70	<i>Cryptococcus curvatus</i>	4.0E-56	61	68
TGTTATCGGT	143	9	8	Heat shock protein 90 homolog	<i>C. albicans</i>	2.0E-32	60	70
GTTTTATGGA	47	3	1	Heat shock protein 60	<i>S. cerevisiae</i>	4.0E-56	69	84
TATACGATAA	46	8	0	Trehalose-6-phosphate synthase	<i>P. ostreatus</i>	7.0E-17	42	51
AAAGAATTAA	28	1	0	Alpha-trehalose-phosphate synthase	<i>S. cerevisiae</i>	1.0E-30	53-75 (3)	80-94 (4)
CATAATTGGC	38	7	3	Putative heat shock protein	<i>Malassezia sympodialis</i>	1.0E-20	35	52
TCAGAAGTTG	122	123	16	Thioredoxin	<i>Coprinus comatus</i>	2.0E-24	47	69

Continued on following page

TABLE 2—Continued

Function and tag	No. of tags detected			BLAST result	Species	E value	% Identity	% Similarity
	In vivo	25°C	37°C					
CAACTTGTTA	57	10	3	Glutathione peroxidase HYR1	<i>S. cerevisiae</i>	2.0E-38	49	63
TGCAAACGCG	31	73	9	Peroxisomal membrane protein Pmp20p	<i>S. pombe</i>	1.0E-21	40	52
CATATCACTG	29	9	2	OV-16 antigen precursor	<i>Onchocerca volvulus</i>	3.0E-11	24	43
CTCTTCATTT	25	11	8	Heat shock protein	<i>S. pombe</i>	2.0E-38	45–63 (2)	72–82 (2)
TAGGCCGTCT	14	23	141	Heat shock protein 10	<i>Cryptocodinium cohnii</i>	3.0E-15	50–77 (3)	75–81 (3)
AACTTAGATC	14	4	4	Heat shock protein 104	<i>Pleurotus sajor-caju</i>	1.0E-161	52–55 (3)	69–79 (3)
<b>Cellular respiration</b>								
TCITTTGATG	115	63	152	ADP, ATP carrier protein	<i>N. crassa</i>	1.0E-118	77–79 (2)	84–88 (2)
ACACGTCTGG	65	92	30	ATP synthase G chain, mitochondrial	<i>S. cerevisiae</i>	7.0E-05	31	50
GGTATTCTAT	54	8	5	Ubiquinol-cytochrome-c reductase	<i>S. cerevisiae</i>	5.0E-06	33	55
TTCGGCAAGG	53	137	114	ADP, ATP carrier protein	<i>N. crassa</i>	1.0E-118	77–79 (2)	84–88 (2)
AACTTTGTTC	41	7	0	Isocitrate dehydrogenase	<i>Coccidioides immitis</i>	2.0E-26	50	59
AGATGAATGG	38	28	0	Cytochrome c oxidase subunit IV	<i>S. pombe</i>	8.0E-16	48	58
AATGGATTAA	32	0	0	Cytochrome P450-like	<i>Nicotiana tabacum</i>	8.0E-25	65	69
GTCGGTGGA	29	140	257	F1 ATPase beta subunit	<i>K. lactis</i>	3.0E-83	80	91
TATTTTTGCA	28	2	0	NADH-ubiquinone oxidoreductase	<i>N. crassa</i>	2.0E-10	37	59
CAAAAACATC	28	3	0	Cytochrome c1 precursor	<i>N. crassa</i>	3.0E-55	54	67
TGAAAACAGT	27	10	0	NADH-cytochrome b5 reductase	<i>Mortierella alpina</i>	5.0E-23	52	65
TAATTTCTAT	25	7	1	3-Hydroxyisobutyrate dehydrogenase	<i>Bacillus subtilis</i>	1.0E-12	27–29 (2)	44–49 (2)
CACATCGTGC	24	20	0	Isocitrate dehydrogenase subunit 1	<i>K. lactis</i>	1.0E-103	50–73 (3)	60–87 (3)
GATACTGTGT	21	3	0	Mitochondrial respiratory chain assembly	<i>S. pombe</i>	1.0E-172	59	71
GCCGGTTATT	21	12	0	64-kDa mitochondrial NADH dehydrogenase	<i>N. crassa</i>	8.0E-28	26–66	68–87
<b>Signal transduction</b>								
CCAATGACGT	67	37	16	GTP-binding nuclear protein Spi1p	<i>S. pombe</i>	3.0E-99	85	93
AACGAATGTA	46	4	0	Rho2 GTP binding protein	<i>Ustilago maydis</i>	7.0E-17	48	65
CAGTTTGTC	36	10	1	Rho GDP dissociation inhibitor alpha	<i>Bos taurus</i>	2.0E-32	40	57
CAGGAGATAT	34	5	1	Small GTP-binding protein	<i>Aspergillus oryzae</i>	5.0E-87	82	91
CAGATCTTCT	31	18	7	Guanine nucleotide-binding protein	<i>N. crassa</i>	1.0E-140	72	85
AATTCGCTAT	22	27	0	14-3-3 protein	<i>S. commune</i>	1.0E-123	96	98
GAAAAGACGT	21	7	0	Cell cycle protein p38-2G4 homolog	<i>Homo sapiens</i>	9.0E-11	37	54
CATTATGTTT	23	4	0	Multi-protein binding factor 1	<i>Yarrowia lipolytica</i>	3.0E-25	47	59
GAGAAAAAAA	19	4	0	Cyclophilin A	<i>Hirudo medicinalis</i>	3.0E-13	52–79 (2)	64–86 (2)
<b>Transport</b>								
TTCAGCAGGC	101	490	96	Putative metal transporter (Zn)	<i>S. pombe</i>	6.0E-52	36	50
CCCATCGTAT	55	21	0	Plasma membrane iron permease	<i>S. pombe</i>	7.0E-14	43	57
CATAGATAAC	32	0	4	Golgi GDP-mannose transporter	<i>C. albicans</i>	2.0E-38	54–60 (2)	67–69 (2)
CTGTTCCGCA	29	12	8	High-affinity copper transporter	<i>S. pombe</i>	2.0E-24	40	53
CAACATAACA	28	11	0	Phosphate transport protein	<i>N. crassa</i>	2.0E-76	50	66
CGAACCCGGC	27	41	75	Pho88p	<i>S. cerevisiae</i>	4.0E-37	47	65
TATCTGATTT	23	23	3	Hexose transporter protein	<i>Aspergillus parasiticus</i>	4.0E-13	38	63
CATATTATGT	14	0	0	Amino acid transporter	<i>Uromyces viciae-fabae</i>	1.0E-119	38–64 (3)	61–78 (3)
<b>Carbohydrate metabolism</b>								
GTCGTAGAGT	146	48	6	Enolase 3 (beta, muscle)	<i>H. sapiens</i>	4.0E-48	69	81
ATTGAATGTA	67	1	0	Alcohol dehydrogenase	<i>B. subtilis</i>	4.0E-22	44	53
CATTACTGCA	63	23	0	Glucose 1-dehydrogenase	<i>B. subtilis</i>	3.0E-36	34–43 (2)	51–62 (2)
TAGTGTCCCG	80	71	16	6-Phosphogluconate dehydrogenase	<i>A. oryzae</i>	0.0E+00	68	79
ATAAGCTTTC	64	162	1	Mannitol-1-phosphate dehydrogenase	Annotated			
AAAAACGCGT	58	109	2	Myo-inositol 1-phosphate synthase	<i>N. crassa</i>	2.0E-67	54	70
CATCCAAAG	51	38	1	UDP-glucose pyrophosphorylase 2	<i>H. sapiens</i>	5.0E-65	61	77
CTTCCTGTTC	49	37	3	Putative phosphoglucomutase	<i>Oryza sativa</i>	2.0E-39	57	74
CAAAATGCAAC	45	5	0	Glycerol-3-phosphate phosphatase	<i>Emericella nidulans</i>	2.0E-22	31	48
AAGTGTGGTA	38	29	2	Transaldolase	<i>S. pombe</i>	1.0E-106	71	82
AAGCTATGAA	36	4	0	Phosphoglyceromutase	<i>A. oryzae</i>	1.0E-27	53	71
CAGACGTAAC	36	49	3	Related to aldo-keto reductase YPR1	<i>N. crassa</i>	9.0E-13	38	59
CATCACTCTT	31	107	3	Pyruvate decarboxylase	<i>Candida glabrata</i>	5.0E-26	52	66
CAAAAGTAGA	29	3	1	Pyruvate carboxylase	<i>P. angusta</i>	1.0E-43	51	62
TTCCCTAATC	29	11	1	Fructose-bisphosphatase	<i>Spinacia oleracea</i>	2.0E-33	76	83
ATTTATCAAA	26	1	0	ATP citrate lyase	<i>S. pombe</i>	5.0E-35	67	76
TGTCAAAAAA	26	38	1	Transaldolase	<i>S. pombe</i>	1.0E-114	68	78
CAGCAGTCAT	26	5	0	Dihydrolipoamide succinyltransferase	<i>A. fumigatus</i>	9.0E-49	69	76
CAGCCAGTGT	26	10	0	Aldehyde dehydrogenase	<i>Agaricus bisporus</i>	7.0E-33	54	67
ACATGGGTTT	25	19	1	Dihydrolipoamide acetyltransferase	<i>C. elegans</i>	4.0E-73	59	76
GCACGGAGAT	22	37	1	6-Phosphogluconolactonase	<i>S. pombe</i>	8.0E-55	44	59
TAAAGCCGTA	20	4	0	2-Keto-3-deoxygluconate oxidoreductase	<i>B. subtilis</i>	6.0E-53	42	55
<b>Amino acid metabolism</b>								
AAGTTTGCCCT	42	5	6	Methylthioadenosine phosphorylase synthesis	<i>S. pombe</i>	6.0E-64	45	61
CATACAGGTC	59	28	2	Glutamine synthetase	Annotated			
CAAAACGAAA	24	10	0	Glycine cleavage system h protein precursor	<i>S. pombe</i>	7.0E-29	56	76
CATCTGTTGA	22	1	1	Homocitrate synthase	<i>Penicillium chrysogenum</i>	3.0E-54	72	83
CCATTGTCAC	21	8	3	Glycine hydroxymethyltransferase-like protein	<i>A. thaliana</i>	6.0E-42	56	67
TGATTATGAA	16	0	0	Glutamine-dependent NAD <sup>+</sup> synthase (Ons1p)	<i>S. cerevisiae</i>	1.0E-116	50	59

Continued on following page



TABLE 2—Continued

Function and tag	No. of tags detected			BLAST result	Species	E value	% Identity	% Similarity
	In vivo	25°C	37°C					
Aromatic compound degradation								
CAAATTCATT	64	7	0	Dienelactone hydrolase family	<i>S. pombe</i>	1.0E-15	30	54
CATTTATGAA	61	17	0	1,4-Benzoquinone reductase	<i>Phanerochaete chrysosporium</i>	2.0E-46	47	61
Cell wall								
ACGTAATATG	50	3	2	Chitin deacetylase-like mannoprotein MP98	Annotated			
GACATTTTGA	56	6	2	Chitin deacetylase	<i>S. commune</i>	5.0E-08	41	60
AACGTCTGCC	29	80	303	Probable membrane protein YLR152c	<i>S. cerevisiae</i>	3.0E-04	35	51
CACAGTGTA	12	5	0	GDP-mannose pyrophosphorylase	<i>A. thaliana</i>	7.0E-76	38–73 (4)	56–94 (4)
Unclassified								
ATATGAAAGA	489	23	21	CipC	<i>E. nidulans</i>	1.0E-08	52–70 (3)	72–76
TAGTCTTTCG	44	57	2	Aldehyde reductase (NADPH)	<i>Sporidiobolus salmonicolor</i>	3.0E-27	40	50
CTCAGCGATG	36	384	198	Cytokine-inducing-glycoprotein	Annotated			
AATTCTTGGC	57	24	2	Myosin heavy chain-like	<i>S. pombe</i>	5.30E-02	29	54
AACCACACTA	34	37	65	Similar to benzodiazepin receptor	<i>X. laevis</i>	1.0E-19	38	52
CGAACAGCTT	31	34	1	YNR018w	<i>S. cerevisiae</i>	2.0E-11	28	48
TAATTTCTAT	25	7	1	Hypothetical oxidoreductase	<i>B. subtilis</i>	1.0E-12	27–29 (2)	44–49 (2)
AATTTGAGTC	20	9	0	Actin-binding protein with SH3 domains	<i>S. pombe</i>	6.0E-08	39–53 (2)	54–72 (2)
CACCAGGCAT	20	42	16	F6	<i>Gossypium hirsutum</i>	1.0E-20	44	69
Nucleotide metabolism								
CAAAATGCAC	23	3	1	Adenosine-5'-phosphosulfate kinase	<i>Penicillium chrysogenum</i>	1.0E-38	58	74
CATCACCGGT	23	20	3	Denylosuccinate synthetase	<i>S. cerevisiae</i>	6.0E-69	57	71
CATATTGAGT	82	59	15	Uracil phosphoribosyltransferase	<i>N. crassa</i>	2.0E-37	65	84
DNA replication								
CATAAAATGA	25	3	0	DNA-directed RNA polymerase II	<i>H. sapiens</i>	8.0E-07	48	81
Chromatin structure								
TATTTCAAGT	42	21	1	Histone H3	<i>M. alpina</i>	3.0E-65	94	97
TGGATGTGGA	35	14	4	Suppressor of mitochondrial histone mutant	<i>N. crassa</i>	5.0E-94	59	71
Lipid and sterol metabolism								
GCCGTTCTTA	40	5	70	Malonyl-CoA decarboxylase	<i>Rattus norvegicus</i>	5.0E-19	65	71
ATTCAAAAAA	35	11	0	ATP citrate-lyase	<i>Ciona intestinalis</i>	2.0E-24	71	82
GATAAGGTGT	20	3	0	Oxysterol-binding protein	<i>S. pombe</i>	5.0E-17	46	54
Nitrogen metabolism								
CAGCGATGGT	34	10	0	Ni-binding urease accessory protein	<i>N. crassa</i>	1.0E-82	63	72
Cytokinesis								
CAGATGGAGA	27	30	75	Tropomyosin	<i>S. pombe</i>	4.0E-06	21–54 (2)	30–70 (2)
RNA interference								
ATCGAAATGC	24	23	0	Argonaute protein	<i>O. sativa</i>	9.0E-19	56	77
Actin polymerization								
TAAGAAGTTT	22	8	0	Actin-capping protein alpha-2 chain	<i>N. crassa</i>	5.0E-15	38–69 (2)	51–80 (2)
Vesicle transport								
AAATCTTATG	22	4	0	Alpha-cop protein	<i>Bos primigenius</i>	1.0E-33	39	57
Vacuole biogenesis								
ATTCCATCTA	20	1	0	VpsA	<i>A. nidulans</i>	1.0E-37	56	78

<sup>a</sup> Numbers have been normalized to the size of the smallest library for comparison (30,468 tags). Tag abundance is presented for each library in shaded boxes in which the shading is proportional to the abundance of that tag such that darker shading corresponds to higher levels of abundance.

<sup>b</sup> Values in parentheses refer to the number of BLAST hits within the proteins that were divided by introns.

The comparison of our in vivo and in vitro data indicated a surprising difference in the regulation of RNA levels for the *HSP60*, *HSP70*, and *HSP90* genes. Specifically, these tags do not appear to be abundant in strain H99 at 37°C. This result supports the hypothesis that serotype A strains of *C. neoformans* such as H99 are not stressed at 37°C, whereas serotype D

strains are stressed at 37°C. The latter observation is corroborated by the fact that transcript levels of *HSP60*, *HSP70*, and *HSP80/90* genes are all elevated at 37°C relative to 25°C in vitro in the serotype D strain B3501A (83). It is possible that the increased body temperature of the rabbit (39.5°C) causes a stress response in the serotype A H99 strain or that there is



some other aspect of in vivo growth conditions that caused the increase in transcript levels for stress response genes in H99. We have been able to show that the induction of *HSP60*, *HSP70*, and *HSP80/90* occurred at 37°C in H99 under low-iron growth conditions (unpublished observations). This supports the hypothesis that the low-iron environment of the host is a key contributing factor in the induction of transcription of these heat shock protein genes in vivo. This difference between serotype A and D strains in temperature stress responses further supports the known differences between serotype A and D strains in their growth abilities at high temperature (57).

In addition to genes that play a role in the response to heat stress, we also identified genes that play a role in oxidative stress. These included genes encoding thioredoxin (67), glutathione peroxidase (40), and a peroxisomal membrane protein. The RNA for the peroxisomal membrane protein is induced in response to four different stress conditions (metal, heat shock, osmotic, and DNA damage stresses) in *Schizosaccharomyces pombe* (20). In *C. neoformans* the tags corresponding to these genes were abundant at 37°C, suggesting a global increase in transcript levels for oxidative stress response genes when cells are placed at higher temperatures. The possibility that the *C. neoformans* cells in the CSF are under stress is further supported by the identification of tags for three enzymes (i.e., trehalose-6-phosphate synthase and two trehalose phosphate synthases) known to be involved in the synthesis of trehalose, the stress-protective sugar. Microarray analysis has shown that these genes are upregulated in *S. cerevisiae* in response to several other stresses besides temperature (18).

The production of stress-related proteins in vivo may be important in protecting the fungus from oxidative radicals produced by macrophages and neutrophils which occur in the CSF of rabbits during meningitis (70). The *C. neoformans* cells that we used were isolated at times of infection in which the number of inflammatory cells would be expected to be the highest in the CSF (although the immune response was suppressed by cortisone treatment in the experiment of Perfect et al. [70]). Previous work has demonstrated that cortisone-treated rabbits develop chronic progressive meningitis that can be fatal after 2 to 12 weeks, and all of the pathological findings in this rabbit model resemble those of fatal human cryptococcal meningitis cases (70). Following infection with a pathogen, the CSF becomes infiltrated with neutrophils and macrophages and, under pathological conditions, monocytes in the CSF are capable of phagocytosis and production of reactive oxygen species (69). It has been shown that the presence of *C. albicans* increases the transcription of genes known to be involved in antioxidant response when exposed to blood and that this response is dependent on the presence of host blood cells rather than the plasma. This is suggestive of a response of *C. albicans* to the production of oxygen radicals from phagocytic cells (33). It is likely that under the conditions found in the rabbit model, *C. neoformans* was responding to oxidative radicals produced by phagocytic cells in the CSF by an upregulation of transcription of oxidative stress response genes.

**Cellular respiration.** *C. neoformans* is considered to be an obligate aerobe, and oxygen is a limiting nutrient for growth in vitro (64). The brain is known to consume 25% of the available oxygen in the body, and oxygen and glucose are rapidly transported from the bloodstream to the CSF. Several tags for genes

encoding mitochondrial proteins (including components of the electron transport chain such as NADH dehydrogenase, different cytochrome c subunits, and ATP synthase subunits) were highly abundant in vivo. Upon comparison with the abundance of the same tags in vitro, it was found that the cytochrome oxidoreductase subunits and the NADH oxidoreductase tags were present in vitro at 25°C but were present at very low levels (or not at all) at 37°C. If transcript abundance can be correlated with protein abundance, then the respiration rate may be higher at lower temperatures in *C. neoformans*.

The abundance of two tags corresponding to two different isocitrate dehydrogenases correlates well with the putative high level of energy requirement of these cells, because this enzyme is associated with the tricarboxylic acid cycle of the mitochondria and is essential for respiration. Together, these results suggest that energy requirements of yeast cells in the CSF are high. This is expected for actively growing and respiring cells, and this result is consistent with abundant expression levels of ribosomal proteins.

**Signal transduction.** Several tags corresponding to genes encoding small G proteins were abundant, including those encoding members of the RAS and RHO superfamilies. Small G proteins play an important role in the development and pathogenesis of fungi. For example, *C. neoformans* Ras1p has been shown to control both the mitogen-activated protein (MAP) kinase cascade and cAMP-PKA signaling pathway and is involved in cross talk between the two pathways (5). Both the cAMP-PKA pathway and a MAP kinase pathway are implicated in regulating morphogenesis and virulence in *C. neoformans* (5, 26, 94). During the induction of filamentous growth in *S. cerevisiae*, a MAP kinase cascade is activated by a RAS protein (Ras2p) (61) and a 14-3-3 protein (Bmh1p) that is highly similar to the 14-3-3 protein identified in our SAGE data (75). Comparison of the abundance of tags for cell signaling genes identified in vivo relative to those identified in vitro showed that seven out of eight tags are most abundant in vivo. Further, six tags displayed a statistically significant ( $P < 0.05$ ) increase in abundance in vivo. These tags correspond to the homologues for a Rho2 GTP-binding protein, Rho GDP-dissociation inhibitor, small GTP-binding protein, 14-3-3 protein, and the multiprotein binding factor. It is not surprising that several genes involved in cell signaling are highly expressed in vivo due to the requirement of signaling pathways in the regulation of ribosomal protein biosynthesis, the cell cycle, the cell stress response, and the production of known virulence factors (melanin and the polysaccharide capsule) (4, 6, 26). The identification of a tag which corresponds to a unique putative cyclophilin A is interesting, because two other cyclophilins have been identified in *C. neoformans* and one of these is important for virulence (93).

**Transport.** Tags corresponding to eight genes that encoded proteins involved in small-molecule transport were identified. These included proteins involved in transport functions for inorganic phosphate, transition metals, and monomeric sugars and an amino acid transporter probably specific for basic amino acids. Transition metals such as copper, iron, and zinc are important for the function of multiple proteins, because they stabilize protein structure and facilitate redox reactions (73). Five of the eight tags for small-molecule transport proteins identified here were abundant in vivo but were found at

low levels in vitro at both temperatures. Exceptions included a putative membrane protein (similar to Pho88p of *S. cerevisiae* and abundant at 25°C) involved in phosphate transport, a putative metal transporter, a probable (as determined on the basis of BLAST searches) zinc transporter (also abundant at 25°C), and a hexose transporter (with similar levels of abundance in vivo and at 25°C). These findings suggest that there is a significant requirement for metals and phosphate during growth in the CSF and that these molecules are limiting. Phosphate is important for energy generation in the mitochondria. The phosphate transporter identified by our SAGE analysis is most similar to phosphate transporters of the mitochondrial carrier family. The increased abundance of a tag corresponding to the phosphate transporter in vivo correlates well with our identification of an increased abundance of tags for genes encoding the electron transport chain. Iron in the CSF is bound to brain-derived transferrin, and the availability of iron for *C. neoformans* is thought to be limited during infection (1).

This finding correlated with the significant increase in the abundance of a tag corresponding to an iron permease gene observed under in vivo conditions relative to in vitro conditions. Zinc is important in the brain, where it functions as a neurotransmitter due to its secretion from synaptic vesicles and interaction with specific receptors. In addition to being temperature regulated (with increased abundance at 25°C), the probable zinc transporter transcript is abundant under all growth conditions. This is similar to what was observed for the same gene in the serotype D strain (83). Glucose transport to the brain occurs at high levels due to the large energy requirement. However, the concentration of glucose in the CSF is lower than that in plasma. This may be related to the presence of a tag that corresponds to a hexose transporter in the top 304 tags found during in vivo growth of *C. neoformans*.

**Carbohydrate metabolism.** One of the most intriguing tags identified a gene encoding mannitol-1-phosphate dehydrogenase. This tag was most abundant in vivo and at 25°C but not at 37°C. The enzyme has also been implicated in the response to heat stress in *C. neoformans* (86), and D-mannitol is produced by *C. neoformans* in the CSF of rabbits during experimental meningitis (97). In fact, the accumulation of mannitol during infection has been correlated with the outcome of meningitis and may act as an antioxidant and/or osmoticum.

A tag for myo-inositol 1-phosphate synthase (*MYO1*) was also identified by our analysis as abundant in vivo. This gene is temperature regulated such that the tag is most abundant at 25°C relative to 37°C, and this is similar to what was observed in the serotype D strain B3501 (83). This finding suggests that the abundance of the *MYO1* gene in vivo is not due to temperature regulation but rather to some other aspect of the in vivo environment. Interestingly, a tag that was found uniquely in vivo relative to in vitro corresponded to an inositol monophosphatase (Table 3). Inositol monophosphatase is involved in the inositol cycle of calcium signaling in *S. cerevisiae* (55). The CSF is known to be an inositol-rich environment (82), and *C. neoformans* is capable of using inositol as a sole carbon and energy source (12). Thus, it is possible that inositol utilization is an important mechanism for survival of *C. neoformans* as a fungal pathogen in the CSF. It has also been shown that inositol phosphoryl ceramide synthase plays a direct role in intracellular growth and melanin production in *C. neoformans* (56).

This also correlated with the identification of a hexose transporter tag abundant in the *C. neoformans* in vivo SAGE library (classified under transporters in Table 2).

Several enzymes identified by our SAGE tags are known to be involved in the pentose-phosphate shunt, including two transaldolases, 6-phosphate gluconate dehydrogenase, and 6-phosphogluconolactonase. The major function of the pentose-phosphate shunt is the generation of NADPH (energy in the form of reducing power) and the supply of ribose-5-phosphates to the cell for nucleic acid synthesis. Cells that are undergoing fatty acid and sterol synthesis also require high amounts of NADH. Furthermore, cells growing rapidly require high rates of nucleic acid synthesis and therefore have a highly active pentose-phosphate shunt. In addition, it has been shown for *S. cerevisiae* that the pentose-phosphate shunt plays a role in the protection of cells against oxidative stresses (41, 80).

The tag for enolase was abundant in vivo relative to the levels of abundance seen at both in vitro temperatures, and the tag displayed temperature-regulated changes in abundance, with a higher level at 25 than at 37°C. In addition to its role in glycolysis, enolase has been implicated as a potent allergen in *Aspergillus fumigatus* (51), *C. albicans* (27), *Pneumocystis carinii*, and *P. ratti* (32). Enolase has been localized to both the cytoplasm and cell wall of *C. albicans* (7), and heat shock does not induce enolase gene expression in this fungus (34). Similarly, our *C. neoformans* SAGE data indicated that transcript levels for the gene are not higher at 37°C. In addition, enolase is involved in plasminogen binding and degradation of host tissues (fibrinolysis) in *P. carinii* and *P. ratti* (32). Thus, the high level of enolase tag abundance in our SAGE library is suggestive of a role in *C. neoformans* pathogenesis.

**Amino acid metabolism.** Several amino acid metabolism genes were identified as abundant in vivo but not in vitro. Two of these genes encoded enzymes such as a glycine cleavage system protein precursor and glycine-hydroxymethyltransferase involved in the mitochondrial glycine cleavage system which mediates the entry of one-carbon units into folate-dependent pathways (45). Reduced folates are found in higher concentrations in the CSF (32 ng/ml) than in the plasma (6.5 ng/ml) (81). In addition to the importance of glycine in the metabolism of one-carbon fragments, peptides, and nucleotides within the cell, free glycine plays an important role in the mammalian brain as a neurotransmitter and neuromodulator such that disruption of glycine metabolism in the brain leads to a severe neurological disorder (49).

**Aromatic compound degradation.** We have identified two tags corresponding to enzymes involved in aromatic compound degradation. Dienelactone hydrolase degrades chlorinated aromatic compounds, and 1,4-benzoquinone reductase is involved in the degradation of the aromatic intermediates produced from lignin degradation in *Phanerochaete chrysosporium*, the wood-rotting basidiomycete fungus (2). It is well documented in the literature that basidiomycete fungi are capable of the degradation of aromatic compounds, and the potential use of these fungi in bioremediation is being explored (72). In the natural environment, these enzymes are important for the degradation of polymeric lignin and its intermediates (such as quinines, hydroquinones, benzaldehydes, benzoic acids, and ring-opened fragments) by *P. chrysosporium* (15). *C. neoformans* may degrade lignin in the environment, and this idea

TABLE 3. Annotated SAGE tags for the top 100 tags that are unique to the in vivo library relative to in vitro

Tag	No. of tags detected in vivo	BLAST result	Species	E value	% Identity	% Similarity	GO biological process
TGATTATGAA	25	Glutamine-dependent NAD <sup>+</sup> synthase	<i>Saccharomyces cerevisiae</i>	1.0E-116	50	59	Amino acid metabolism
CATAATTATGT	22	Hypothetical protein	<i>Neurospora crassa</i>	1.0E-24	46	75	Uncharacterized
TAICTATGTGA	18	Receptor-associated protein	<i>Schizosaccharomyces pombe</i>	1.0E-13	40	62	Antiapoptosis
CAITTTGTATA	17	G10 protein homolog	<i>Pleurotus ostreatus</i>	2.0E-42	85	96	mRNA splicing
CCAAITGATTA	17	Aconitase protein	<i>Bacteroides fragilis</i>	3.0E-06	50	75	Carbohydrate metabolism
GACATATGAA	17	Alpha-amylase	<i>Debaryomyces occidentalis</i>	1.0E-21	33	55	Carbohydrate metabolism
TGTTATATGA	17	Inositol monophosphatase	<i>Rattus norvegicus</i>	1.0E-37	39-44	59-61	Carbohydrate metabolism
GAGAGTGTGA	16	VHS domain protein	<i>S. pombe</i>	5.0E-17	33	52	Vesicle transport
AITAGTTAAT	15	Clathrin coat assembly protein	<i>S. pombe</i>	5.0E-19	40-53 (3) <sup>a</sup>	58-79 (3)	Vesicle transport
TAACATACAT	15	Oligosaccharyltransferase subunit	<i>Mus musculus</i>	3.0E-05	31-63 (3)	41-72 (3)	Antiapoptosis
ATTATAACGA	14	Proteasome component PUP2	<i>S. pombe</i>	2.0E-27	60-95 (2)	74-95 (2)	Protein catabolism
AITCACAGGA	14	Regulatory particle non-ATPase; Rpn9p	<i>S. cerevisiae</i>	8.0E-21	46	68	Protein catabolism
CATAITATGT	14	Amino acid transporter	<i>Uromyces viciae fabae</i>	1.0E-119	38-64 (3)	61-78 (3)	Transport
CATCTTAGAT	13	UMP-CMP kinase	<i>Leptinula edodes</i>	7.0E-50	65	80	Signal transduction
TAITCTACAC	13	Predicted protein	<i>N. crassa</i>	8.0E-12	45	57	Uncharacterized
AITTTACAGAA	12	Dynammin-related protein	<i>S. pombe</i>	3.0E-16	50	69	Mitochondrial organization-biogenesis
CATAGAAITTA	12	RNA polymerase II subunit RPB9	<i>S. cerevisiae</i>	4.0E-07	48	63	Transcription
GAATTGATAG	12	Arc1p	<i>S. cerevisiae</i>	2.0E-18	44	58	Amino acid metabolism
TACTTCTTGA	12	Related to BET1 protein	<i>N. crassa</i>	1.0E-09	34	52	Vesicle transport
AATTATTAT	11	Hypothetical protein	<i>S. pombe</i>	2.0E-06	24	45	Uncharacterized
GGTCAGTCGA	11	Hypothetical protein	<i>Plasmodium yoelii yoelii</i>	1.0E-17	72-77 (2)	85-89 (2)	Uncharacterized
TAITTCATTT	11	U3 small nuclear RNP protein IMP3	<i>S. cerevisiae</i>	9.0E-50	59	74	RNA splicing
TTATGGGTAG	11	Bud20p	<i>S. cerevisiae</i>	7.0E-11	44	57	Nuclear pore
AAATGTAITAA	10	Stomatin-like protein	<i>Gibberella fujikuroi</i>	2.0E-13	57-63 (2)	72-79 (2)	Cell wall maintenance
CAATCAATAT	10	FKBP-70; immunophilin	<i>S. cerevisiae</i>	9.0E-39	70	81	Protein biosynthesis
CATAGATGCC	10	Hypothetical protein	<i>N. crassa</i>	5.0E-11	35	54	Uncharacterized
CAITTTACT	10	NADH/ubiquinone oxidoreductase	<i>N. crassa</i>	2.0E-45	63	78	Cellular respiration
CAITTTGACT	10	Ribosomal protein L27	<i>Filobasidium floriforme</i>	5.0E-77	84	85	Protein biosynthesis
TTTATAGATC	10	Mitochondrial carrier	<i>N. crassa</i>	3.0E-53	67	78	Mitochondrial organization-biogenesis

<sup>a</sup> Values in parentheses refer to the number of BLAST hits within the proteins that were divided by introns.



correlates well with the natural tree habitat for *C. neoformans* (74). Our observed abundance of the corresponding SAGE tags in vivo suggests a possible requirement for similar functions during *C. neoformans* infection of the mammalian host.

**Cell wall.** One tag identified the gene for *C. neoformans* MP98, an intriguing secreted mannoprotein that shows similarity to chitin deacetylases and that probably stimulates the T-cell response (39). Chitin deacetylases hydrolyze N-aceto-amido bonds of chitin during cell wall formation. Chitin deacetylase is also thought to play a role in plant-pathogen interaction involving the fungus *Colletotrichum lindemuthianum*; the enzyme is extracellular in this case and acts on chitin oligomers that induce plant defense mechanisms (11, 44, 89, 90). Along with the high transcript level of the MP98 gene, a second chitin deacetylase gene (GACATTTTGA) was also abundant in vivo. Both of the tags for these genes did not show significant abundance under in vitro growth conditions, emphasizing their possible importance in vivo. The identification of a tag that corresponded to a GDP-mannose pyrophosphorylase is interesting in the context of capsule biosynthesis in *C. neoformans*, because mannose is the main component of sugar backbone of the capsule (14). This also may be related to the identification of the Golgi-GDP mannose transporter classified under the GO term heading of transport. Both of these tags were most abundant under in vivo growth conditions relative to in vitro growth conditions.

**Unclassified.** Two poorly characterized proteins have been identified by our SAGE data as potentially important in pathogenesis. The CipC protein was originally identified in *Aspergillus nidulans* as a protein that is produced in high amounts in the presence of the antifungal agent concanamycin A (59). Expression of the *C. neoformans* *CIPC* gene in the serotype D strain B3501A is induced 55-fold at 37°C relative to levels seen at 25°C (83). We did not observe similar temperature regulation for the serotype A strain; however, the abundance of the tag for this gene was significantly elevated in vivo relative to that seen in vitro and represents the third-most-abundant tag in our in vivo SAGE library. This result strongly implicates this gene as serving an important role during growth in vivo. We have knocked out the *CIPC* gene in the B3501A strain and found that mutants exhibited a temperature-sensitive growth phenotype (B. Steen, unpublished results). The gene for the second protein was already described in GenBank (AJ345095) as encoding cytokine-inducing glycoprotein. The tag for this gene was abundant under in vitro growth conditions at both 25 and 37°C, and it was found to be one of the most abundant tags when *C. neoformans* cells were growing in vivo.

A SAGE tag (identifying a gene with similarity to the entire OV-16 antigen of *Onchocerca volvulus*, the causative agent of onchocerciasis [“river blindness”], which affects 18 million Africans and Latin Americans) was also unclassified. OV-16 antigen is highly immunogenic during the early stages of infection prior to the detection of the parasite (54). It is interesting that the gene for this protein exists in *C. neoformans*.

**Transcripts that are unique to the in vivo library.** From the list of tags that are unique to the in vivo library relative to those in the temperature in vitro libraries, we have annotated the 100 most abundant tags. Of these tags, we found that 29 did not match any H99 genomic contigs at the Duke Center for Genome Technology or at the Whitehead Institute Center for

Genome Research or any ESTs at The University of Oklahoma, four tags matched more than one contig, and 35 tags had no significant BLAST results at NCBI. Of the 29 tags that did not hit a corresponding EST or genomic sequence, 7 were due to rabbit sequences from contaminating rabbit cells from the CSF, as determined by searches of rabbit ESTs and the genomic sequence. This suggests that the uniqueness of 7% of the tags in the in vivo library was due to the presence of rabbit sequences. It is also possible that these tags correspond to sequences currently not available in existing H99 databases. That 35% of the tags were found to correspond to gene sequences without a BLAST result at NCBI suggested the existence of a large subset of undiscovered genes that were expressed by the fungus during growth in the host CSF. Investigations of the remaining 24 tags resulted in annotations that could be classified under different previously discussed categories, such as protein biosynthesis, protein catabolism, cellular respiration, signal transduction, and cell wall maintenance (Table 3). In addition, tags that were classified under new categories, including genes with predicted roles in anti-apoptosis, mRNA splicing, vesicle transport, mitochondrial organization, and biogenesis and transcription, were identified. A nuclear pore protein was also identified. The unique expression suggests specific roles for these functions during growth of *C. neoformans* in the CSF of rabbits.

**Conclusions.** Our work explored the hypothesis that genes that are turned on or expressed at high levels during infection belong to genetic pathways or networks important for survival and the progression of infection during rabbit cryptococcal meningitis. In this context, we identified several functions that are potentially important during infection, including protein catabolism, the heat stress response, and the oxidative stress response. Additionally, we identified abundant transcripts for genes involved in nutrient acquisition and transport that provide clues about metabolic limitations for *C. neoformans* growth in the CSF. Our SAGE data also confirmed in vivo abundance for some previously identified genes with suggested roles in infection. These included genes for MP98, mannitol dehydrogenase, heat shock proteins, enolase, and myo-inositol phosphate synthase. These results help to validate SAGE as a discovery tool to understand the infection process and to identify potential antifungal drug targets or strategies. We are now pursuing functional tests to examine the roles of selected genes identified by our work. In particular, we are interested in studying the roles of the *CIPC* and *HSP12* orthologs because of their high transcript levels. We are also targeting functions that may be key for nutrient acquisition, including the proteases and the transporters. Finally, we believe that our findings will be an important resource for the medical mycology research community and will form a strong foundation for more detailed explorations of fungal gene expression during infection.

#### ACKNOWLEDGMENTS

We thank the *C. neoformans* cDNA Sequencing Project at The University of Oklahoma (Bruce A. Roe, Doris Kupfer, Heather Bell, Sun So, Yuong Tang, Jennifer Lewis, Sola Yu, Kent Buchanan, Dave Dyer, and Juneann Murphy) for access to the EST information that was essential in the analysis of the SAGE data. We also thank Fred Dietrich at the Duke Center for Genome Technology for access to the Duke University database for H99 genome sequence. We are grateful to the Whitehead Institute/MIT Center for Genome Research (

//www-genome.wi.mit.edu) for access to genomic sequence data. Thanks also to Cletus D'Souza for critical review of the manuscript, Aliya Hasham for SAGE data analysis, Kristin Tangen for her SAGE information for H99 grown in low-iron conditions, and Tian Lian and Kim MacDonald for their work with the temperature libraries.

This work was funded by a Scholar Award (to J.K.) from the Burroughs Wellcome Fund and by Public Health Service grant AI28388 (J.R.P.). Additional funding was obtained from the Canadian Institutes of Health Research. M. Marra and S. J. M. Jones are Biomedical Scholars of the Michael Smith Foundation for Health Research.

#### REFERENCES

- Ahluwalia, M., E. Brummer, S. Sridhar, R. Singh, and D. A. Stevens. 2001. Isolation and characterisation of an anticytotoxic protein in human cerebrospinal fluid. *J. Med. Microbiol.* **50**:83–89.
- Akilesvaran, L., B. J. Brock, J. L. Cereghino, and M. H. Gold. 1999. 1,4-Benzoquinone reductase from *Phanerochaete chrysosporium*: cDNA cloning and regulation of expression. *Appl. Environ. Microbiol.* **65**:415–421.
- Alspaugh, J. A., L. M. Cavallo, J. R. Perfect, and J. Heitman. 2000. RAS1 regulates filamentation, mating and growth at high temperature of *Cryptococcus neoformans*. *Mol. Microbiol.* **36**:352–365.
- Alspaugh, J. A., J. R. Perfect, and J. Heitman. 1997. *Cryptococcus neoformans* mating and virulence are regulated by the G-protein alpha subunit GPA1 and cAMP. *Genes Dev.* **11**:3206–3217.
- Alspaugh, J. A., J. R. Perfect, and J. Heitman. 1998. Signal transduction pathways regulating differentiation and pathogenicity of *Cryptococcus neoformans*. *Fungal Genet. Biol.* **25**:1–14.
- Alspaugh, J. A., R. Pukkila-Worley, T. Harashima, L. M. Cavallo, D. Funnel, G. M. Cox, J. R. Perfect, J. W. Kronstad, and J. Heitman. 2002. Adenylyl cyclase functions downstream of the G-alpha protein Gpa1 and controls mating and pathogenicity of *Cryptococcus neoformans*. *Eukaryot. Cell* **1**:75–84.
- Angiolella, L., M. Facchin, A. Stringaro, B. Maras, N. Simonetti, and A. Cassone. 1996. Identification of a glucan-associated enolase as a main cell wall protein of *Candida albicans* and an indirect target of lipopeptide antimicrobics. *J. Infect. Dis.* **173**:684–690.
- Aoki, S., S. Ito-Kuwa, K. Nakamura, J. Kato, K. Ninomiya, and V. Vidotto. 1994. Extracellular proteolytic activity of *Cryptococcus neoformans*. *Mycopathologia* **128**:143–150.
- Ashburner, M., C. A. Ball, J. A. Blake, D. Botstein, H. Butler, J. M. Cherry, A. P. Davis, K. Dolinski, S. S. Dwight, J. T. Eppig, M. A. Harris, D. P. Hill, L. Issel-Tarver, A. Kasarskis, S. Lewis, J. C. Matese, J. E. Richardson, M. Ringwald, G. M. Rubin, G. Sherlock, and The Gene Ontology Consortium. 2000. Gene ontology: tool for the unification of biology. *Nat. Genet.* **25**:25–29.
- Audic, S., and J.-M. Claverie. 1997. The significance of digital gene expression profiles. *Genome Res.* **7**:986–995.
- Elber, M. S., R. E. Bertram, and J. P. Ride. 1989. Chitin oligosaccharides elicit lignification in wounded wheat leaves. *Physiol. Mol. Plant Pathol.* **34**:3–12.
- Barnett, J. A. 1976. The utilization of sugars by yeasts. *Adv. Carbohydr. Chem. Biochem.* **32**:125–234.
- Blackshaw, S., W. P. Kuo, P. J. Park, M. Tsujikawa, J. M. Gunnerson, H. S. Scott, W. M. Boon, S. S. Tan, and C. L. Cepko. 2003. MicroSAGE is highly representative and reproducible but reveals major differences in gene expression among samples obtained from similar tissues. *Genome Biol.* **4**:R17.
- Bose, I., A. J. Reese, J. J. Ory, G. Janbon, and T. L. Doering. 2003. A yeast under cover: the capsule of *Cryptococcus neoformans*. *Eukaryot. Cell* **2**:655–663.
- Buswell, J. A., and E. Odier. 1987. Lignin degradation. *Crit. Rev. Biotechnol.* **6**:1–60.
- Cardenas, M. E., N. S. Cutler, M. C. Lorenz, C. J. Di Como, and J. Heitman. 1999. The TOR signaling cascade regulates gene expression in response to nutrients. *Genes Dev.* **13**:3271–3279.
- Casadevall, A., and J. R. Perfect. 1998. *Cryptococcus neoformans*. ASM Press, Washington, D.C.
- Causton, H. C., B. Ren, S. S. Koh, C. T. Harbison, E. Kanin, E. G. Jennings, T. I. Lee, H. L. True, E. S. Lander, and R. A. Young. 2001. Remodeling of yeast genome expression in response to environmental changes. *Mol. Biol. Cell* **12**:323–377.
- Chang, W. L., H. C. van der Hyde, and B. S. Klein. 1998. Flow cytometric quantitation of yeast a novel technique for use in animal model work and in vitro immunologic assays. *J. Immunol. Methods* **211**:51–53.
- Chen, D., W. M. Toone, J. Mata, R. Lyne, G. Burns, K. Kivinen, A. Brazma, N. Jones, and J. Bahler. 2003. Global transcriptional responses of fission yeast to environmental stress. *Mol. Biol. Cell* **14**:214–229.
- Chen, L.-C., E. S. Blank, and A. Casadevall. 1996. Extracellular proteinase activity of *Cryptococcus neoformans*. *Clin. Diagn. Lab. Immunol.* **3**:570–574.
- Cox, G. M., H. C. McDade, S. C. Chen, S. C. Tucker, M. Gottfredsson, L. C. Wright, T. C. Sorrell, S. D. Leidich, A. Casadevall, M. A. Ghannoum, and J. R. Perfect. 2001. Extracellular phospholipase activity is a virulence factor for *Cryptococcus neoformans*. *Mol. Microbiol.* **39**:166–175.
- Curiel, T. J., J. R. Perfect, and D. T. Durack. 1982. Leukocyte subpopulations in cerebrospinal fluid of normal rabbits. *Lab. Anim. Sci.* **32**:622–624.
- Davson, H., K. Welch, and M. B. Segal. 1987. The physiology and pathophysiology of the cerebrospinal fluid. Churchill Livingstone, Edinburgh, United Kingdom.
- Deepe, G. S. J., and R. S. Gibbons. 2002. Cellular and molecular regulation of vaccination with heat shock protein 60 from *Histoplasma capsulatum*. *Infect. Immun.* **70**:3759–3767.
- D'Souza, C. A., J. A. Alspaugh, C. Yue, T. Harashima, G. M. Cox, J. R. Perfect, and J. Heitman. 2001. Cyclic AMP-dependent protein kinase controls virulence of the fungal pathogen *Cryptococcus neoformans*. *Mol. Cell. Biol.* **21**:3179–3191.
- Eroles, P., M. Sentandreu, M. V. Elorza, and R. Sentandreu. 1997. The highly immunogenic enolase and Hsp70p are adventitious *Candida albicans* cell wall proteins. *Microbiology* **143**:313–320.
- Ewing, B., and P. Green. 1998. Base-calling of automated sequencer traces using Phred. II. Error probabilities. *Genome Res.* **8**:186–194.
- Ewing, B., L. Hillier, M. C. Wendl, and P. Green. 1998. Base-calling of automated sequencer traces using Phred. I. Accuracy assessment. *Genome Res.* **8**:175–185.
- Feldmesser, M., Y. Kress, P. Novikoff, and A. Casadevall. 2000. *Cryptococcus neoformans* is a facultative intracellular pathogen in murine pulmonary infection. *Infect. Immun.* **68**:4225–4237.
- Finley, D., B. Bartel, and A. Varshavsky. 1989. The tails of ubiquitin precursors are ribosomal proteins whose fusion to ubiquitin facilitates ribosome biogenesis. *Nature* **338**:394–401.
- Fox, D., and A. G. Smulian. 2001. Plasminogen-binding activity of enolase in the opportunistic pathogen *Pneumocystis carinii*. *Med. Mycol.* **39**:495–507.
- Fradin, C., M. Kretschmar, T. Nichterlein, C. Gaillardin, C. d'Enfert, and B. Hube. 2003. Stage-specific gene expression of *Candida albicans* in human blood. *Mol. Microbiol.* **47**:1523–1543.
- Franklyn, K. M., and J. R. Warmington. 1994. The expression of *Candida albicans* enolase is not heat shock inducible. *FEMS Microbiol. Lett.* **118**:219–225.
- Garrido, C., S. Gurbuxani, L. Ravagnan, and G. Kroemer. 2001. Heat shock proteins: endogenous modulators of apoptotic cell death. *Biochem. Biophys. Res. Commun.* **286**:433–442.
- Gordon, D., C. Abajian, and P. Green. 1998. Consed: a graphical tool for sequence finishing. *Genome Res.* **8**:195–202.
- Hershko, A., and A. Ciechanover. 1998. The ubiquitin system. *Annu. Rev. Biochem.* **67**:425–479.
- Holmes, A. R., A. Collings, K. J. Farnden, and M. G. Shepherd. 1989. Ammonium assimilation by *Candida albicans* and other yeasts: evidence for activity of glutamate synthase. *J. Gen. Microbiol.* **135**:1423–1430.
- Huang, C., S.-H. Nong, M. K. Mansour, C. A. Specht, and S. M. Levitz. 2002. Purification and characterization of a second immunoreactive mannoprotein from *Cryptococcus neoformans* that stimulates T-cell responses. *Infect. Immun.* **70**:5485–5493.
- Inoue, Y., T. Matsuda, K.-I. Sugiyama, S. Izawa, and A. Kimura. 1999. Genetic analysis of glutathione peroxidase in oxidative stress response of *Saccharomyces cerevisiae*. *J. Biol. Chem.* **274**:27002–27009.
- Juhnke, H., B. Krems, P. Kotter, and K. D. Entian. 1996. Mutants that show increased sensitivity to hydrogen peroxide reveal an important role for the pentose phosphate pathway in protection of yeast against oxidative stress. *Mol. Gen. Genet.* **252**:456–464.
- Takeya, H., H. Udono, N. Ikuno, Y. Yamamoto, K. Mitsutake, T. Miyazaki, K. Tomono, H. Koga, T. Tashiro, E. Nakayama, and S. Kohno. 1997. A 77-kilodalton protein of *Cryptococcus neoformans*, a member of the heat shock protein 70 family, is a major antigen detected in the sera of mice with pulmonary cryptococcosis. *Infect. Immun.* **65**:1653–1658.
- Takeya, H., H. Udono, S. Maesaki, E. Sasaki, S. Kawamura, M. A. Hossain, Y. Yamamoto, T. Sawai, M. Fukuda, K. Mitsutake, Y. Miyazaki, K. Tomono, T. Tashiro, E. Nakayama, and S. Kohno. 1999. Heat shock protein 70 (hsp70) as a major target of the antibody response in patients with pulmonary cryptococcosis. *Clin. Exp. Immunol.* **115**:485–490.
- Kauss, H., W. Jeblick, and H. Domard. 1989. The degree of polymerization and N-acetylation of chitosan determines its ability to elicit callose formation in suspension cells and protoplast *Catharanthus roseus*. *Planta* **178**:385–392.
- Kikuchi, G. 1973. The glycine cleavage system: composition, reaction mechanism and physiological significance. *Mol. Cell. Biochem.* **1**:169–173.
- Klein, C., and K. Struhl. 1994. Protein kinase A mediates growth-regulated expression of yeast ribosomal protein genes by modulating RAP1 transcriptional activity. *Mol. Cell. Biol.* **14**:1920–1928.
- Kozel, T. R. 1993. Opsonization and phagocytosis of *Cryptococcus neoformans*. *Arch. Med. Res.* **24**:211–218.
- Kozel, T. R., G. S. Pfommer, A. S. Guerlain, B. A. Highison, and G. J. Highison. 1988. Role of the capsule in phagocytosis of *Cryptococcus neoformans*. *Rev. Infect. Dis.* **10**(Suppl. 2):S436–S439.
- Kure, S., K. Tada, and K. Narisawa. 1997. Nonketotic hyperglycinemia:

- biochemical, molecular, and neurological aspects. *Jpn. J. Hum. Genet.* **42**: 13–22.
50. **Kwon-Chung, K. J., and J. C. Rhodes.** 1986. Encapsulation and melanin formation as indicators of virulence in *Cryptococcus neoformans*. *Infect. Immun.* **51**:218–223.
  51. **Lai, H. Y., M. F. Tam, R. B. Tang, H. Chou, C. Y. Chang, J. J. Tsai, and H. D. Shen.** 2002. cDNA cloning and immunological characterization of a newly identified enolase allergen from *Penicillium citrinum* and *Aspergillus fumigatus*. *Int. Arch. Allergy Immunol.* **127**:181–190.
  52. **Lee, S. C., A. Casadevall, and D. W. Dickson.** 1996. Immunohistochemical localization of capsular polysaccharide antigen in the central nervous system cells in cryptococcal meningoencephalitis. *Am. J. Pathol.* **148**:1267–1274.
  53. **Li, Y., R. D. Moir, I. K. Sethy-Coraci, J. R. Warner, and I. M. Willis.** 2000. Repression of ribosome and tRNA synthesis in secretion-defective cells is signaled by a novel branch of the cell integrity pathway. *Mol. Cell. Biol.* **20**:3843–3851.
  54. **Lobos, E., N. Weiss, M. Karam, H. R. Taylor, E. A. Ottesen, and T. B. Nutman.** 1991. An immunogenic *Onchocerca volvulus* antigen: a specific and early marker of infection. *Science* **251**:1603–1605.
  55. **Lopez, F., M. Leube, R. Gil-Mascarell, J. P. Navarro-Avino, and R. Serrano.** 1999. The yeast inositol monophosphatase is a lithium- and sodium-sensitive enzyme encoded by a non-essential gene pair. *Mol. Microbiol.* **31**:1255–1264.
  56. **Luberto, C., D. L. Toffaletti, E. A. Wills, S. C. Tucker, A. Casadevall, J. R. Perfect, Y. A. Hannun, and M. Del Poeta.** 2001. Roles for inositol-phosphoryl ceramide synthase 1 (*IPC1*) in pathogenesis of *Cryptococcus neoformans*. *Genes Dev.* **15**:201–212.
  57. **Martinez, L. R., J. Garcia-Rivera, and A. Casadevall.** 2001. *Cryptococcus neoformans* var. *neoformans* (serotype D) strains are more susceptible to heat than *C. neoformans* var. *grubii* (serotype A) strains. *J. Clin. Microbiol.* **39**:3365–3367.
  58. **Matthews, R., and J. Burnie.** 1992. The role of hsp90 in fungal infection. *Immunol. Today* **13**:345–348.
  59. **Melin, P., J. Schnurer, and E. G. Wagner.** 2002. Proteome analysis of *Aspergillus nidulans* reveals proteins associated with the response to the antibiotic concanamycin A, produced by *Streptomyces* species. *Mol. Genet. Genomics* **267**:695–702.
  60. **Mizuta, K., and J. R. Warner.** 1994. Continued functioning of the secretory pathways is essential for ribosome synthesis. *Mol. Cell. Biol.* **14**:2493–2502.
  61. **Mosch, H.-U., E. Kubler, S. Krappmann, G. R. Fink, and G. H. Braus.** 1999. Crosstalk between the Ras2p-controlled mitogen-activated protein kinase and cAMP pathways during invasive growth of *Saccharomyces cerevisiae*. *Mol. Biol. Cell* **10**:1325–1335.
  62. **Nosanchuk, J. D., B. L. Gomez, S. Youngchim, S. Diez, P. Aisen, R. M. Zancoppe-Oliveira, A. Restrepo, A. Casadevall, and A. J. Hamilton.** 2002. *Histoplasma capsulatum* synthesizes melanin-like pigments in vitro and during mammalian infection. *Infect. Immun.* **70**:5124–5131.
  63. **Nosanchuk, J. D., A. L. Rosas, S. C. Lee, and A. Casadevall.** 2000. Melaninisation of *Cryptococcus neoformans* in human brain tissue. *Lancet* **355**:2049–2050.
  64. **Odds, F. C., T. De Backer, G. Dams, L. Vranckx, and F. Woestenborghs.** 1995. Oxygen as limiting nutrient for growth of *Cryptococcus neoformans*. *J. Clin. Microbiol.* **33**:995–997.
  65. **Odom, A., S. Muir, E. Lim, D. L. Toffaletti, J. R. Perfect, and J. Heitman.** 1997. Calcineurin is required for virulence of *Cryptococcus neoformans*. *EMBO J.* **16**:2576–2589.
  66. **Parcellier, A., S. Gurbuxani, E. Schmitt, E. Solary, and C. Garrido.** 2003. Heat shock proteins, cellular chaperones that modulate mitochondrial cell death pathways. *Biochem. Biophys. Res. Commun.* **304**:505–512.
  67. **Pedrajas, J. R., E. Kosmidou, A. Miranda-Vizuete, J.-A. Gustafsson, A. P. H. Wright, and G. Spyrou.** 1999. Identification and functional characterization of a novel mitochondrial thioredoxin system in *Saccharomyces cerevisiae*. *J. Biol. Chem.* **274**:6366–6373.
  68. **Perfect, J. R., and A. Casadevall.** 2002. Cryptococcosis. *Infect. Dis. Clin. N. Am.* **16**:837–874, v-vi.
  69. **Perfect, J. R., M. M. Hobbs, D. L. Granger, and D. T. Durack.** 1988. Cerebrospinal fluid macrophage response to experimental cryptococcal meningitis: relationship between in vivo and in vitro measurements of cytotoxicity. *Infect. Immun.* **56**:849–854.
  70. **Perfect, J. R., D. R. Selwyn, M. B. Lang, and D. T. Durack.** 1980. Chronic cryptococcal meningitis, a new experimental model in rabbits. *Am. J. Pathol.* **101**:177–194.
  71. **Perfect, J. R., B. Wong, Y. C. Chang, K. J. Kwon-Chung, and P. R. Williamson.** 1998. *Cryptococcus neoformans*: virulence and host defences. *Med. Mycol.* **36**(Suppl. 1):79–86.
  72. **Pointing, S. B.** 2001. Feasibility of bioremediation by white-rot fungi. *Appl. Microbiol. Biotechnol.* **57**:20–33.
  73. **Radisky, D., and J. Kaplan.** 1999. Regulation of transition metal transport across the yeast plasma membrane. *J. Biol. Chem.* **274**:4481–4484.
  74. **Randhawa, H. S., A. Y. Mussa, and Z. U. Khan.** 2001. Decaying wood in tree trunk hollows as a natural substrate for *Cryptococcus neoformans* and other yeast-like fungi of clinical interest. *Mycopathologia* **151**:63–69.
  75. **Roberts, R., H.-U. Mosch, and G. R. Fink.** 1997. 14-3-3 proteins are essential for RAS/MAPK cascade signaling during pseudohyphal development in *Saccharomyces cerevisiae*. *Cell* **89**:1055–1065.
  76. **Rodrigues, M. L., F. C. G. dos Reis, R. Puccia, L. R. Travassos, and C. S. Alviano.** 2003. Cleavage of human fibronectin and other basement membrane-associated proteins by a *Cryptococcus neoformans* serine protease. *Microb. Pathog.* **34**:65–71.
  77. **Salas, S. D., J. E. Bennett, K. J. Kwon-Chung, J. R. Perfect, and P. R. Williamson.** 1996. Effect of the laccase gene *CNLAC1*, on virulence of *Cryptococcus neoformans*. *J. Exp. Med.* **184**:377–386.
  78. **Scheckelhoff, M., and G. S. Deepe, Jr.** 2002. The protective immune response to heat shock protein 60 of *Histoplasma capsulatum* is mediated by a subset of V beta 8.1/8.2<sup>+</sup> T cells. *J. Immunol.* **169**:5818–5826.
  79. **Shamji, A. F., F. G. Kuruvilla, and S. L. Schreiber.** 2000. Partitioning the transcriptional program induced by rapamycin among the effectors of the Tor proteins. *Curr. Biol.* **10**:1574–1581.
  80. **Slekar, K. H., D. J. Kosman, and V. C. Culotta.** 1996. The yeast copper/zinc superoxide dismutase and the pentose phosphate pathway play overlapping roles in oxidative stress protection. *J. Biol. Chem.* **271**:28831–28836.
  81. **Spector, R., and A. V. Lorenzo.** 1975. Folate transport in the central nervous system. *Am. J. Physiol.* **229**:777–782.
  82. **Spector, R., and A. V. Lorenzo.** 1975. Myo-inositol transport in the central nervous system. *Am. J. Physiol.* **228**:1510–1518.
  83. **Steen, B. R., T. Lian, S. Zuyderduyn, W. K. MacDonald, M. Marra, S. J. Jones, and J. W. Kronstad.** 2002. Temperature-regulated transcription in the pathogenic fungus *Cryptococcus neoformans*. *Genome Res.* **12**:1386–1400.
  84. **Stephen, C., S. Lester, W. Black, M. Fyfe, and W. Raverty.** 2002. Multispecies outbreak of cryptococcosis on southern Vancouver Island, British Columbia. *Can. Vet. J.* **43**:792–794.
  85. **Stern, M. D., S. V. Anisimov, and K. R. Boheler.** 2003. Can transcriptome size be estimated from SAGE catalogs? *Bioinformatics* **19**:443–448.
  86. **Suvarna, K., A. Bartiss, and B. Wong.** 2000. Mannitol-1-phosphate dehydrogenase from *Cryptococcus neoformans* is a zinc-containing long-chain alcohol/polyol dehydrogenase. *Microbiology* **146**:2705–2713.
  87. **Thomas, P. W., E. E. Wyckoff, E. J. Pishko, J. J. Yu, T. N. Kirkland, and G. T. Cole.** 1997. The HSP60 gene of the human pathogenic fungus *Coccidioides immitis* encodes a T-cell reactive protein. *Gene* **199**:83–91.
  88. **Trendelenburg, G., K. Prass, J. Priller, K. Kapinya, A. Polley, C. Muselmann, K. Ruscher, U. Kannbley, A. O. Schmitt, S. Castell, F. Wiegand, A. Meisel, A. Rosenthal, and U. Dirnagl.** 2002. Serial analysis of gene expression identifies metallothionein-II as major neuroprotective gene in mouse focal cerebral ischemia. *J. Neurosci.* **22**:5879–5888.
  89. **Tsigos, I., and V. Bouriotis.** 1995. Purification and characterization of chitin deacetylase from *Colletotrichum lindemuthianum*. *J. Biol. Chem.* **270**:26286–26291.
  90. **Vander, P., K. M. Varum, A. Domard, N. E. El Gueddari, and B. M. Moerschbacher.** 1998. Comparison of the ability of partially N-acetylated chitosans and chitoooligosaccharides to elicit resistance reactions in wheat leaves. *Plant Physiol.* **118**:1353–1359.
  91. **Velculescu, V. E., L. Zhang, B. Vogelstein, and K. W. Kinzler.** 1995. Serial analysis of gene expression. *Science* **270**:484–487.
  92. **Velculescu, V. E., L. Zhang, W. Zhou, J. Vogelstein, M. A. Basrai, D. E. Bassett, Jr., P. Hieter, B. Vogelstein, and K. W. Kinzler.** 1997. Characterization of the yeast transcriptome. *Cell* **88**:243–251.
  93. **Wang, P., M. E. Cardenas, G. M. Cox, J. R. Perfect, and J. Heitman.** 2001. Two cyclophilin A homologues with shared and distinct functions important for growth and virulence of *Cryptococcus neoformans*. *EMBO Rep.* **2**:511–518.
  94. **Wang, P., and J. Heitman.** 1999. Signal transduction cascades regulating mating, filamentation, and virulence in *Cryptococcus neoformans*. *Curr. Opin. Microbiol.* **2**:358–362.
  95. **Wang, Y., P. Aisen, and A. Casadevall.** 1995. *Cryptococcus neoformans* melanin and virulence: mechanism of action. *Infect. Immun.* **63**:3131–3136.
  96. **Wang, Y., P. Aisen, and A. Casadevall.** 1996. Melanin, melanin “ghosts,” and melanin composition in *Cryptococcus neoformans*. *Infect. Immun.* **64**:2420–2424.
  97. **Wong, B., J. R. Perfect, S. Beggs, and K. A. Wright.** 1990. Production of the hexitol D-mannitol by *Cryptococcus neoformans* in vitro and in rabbits with experimental meningitis. *Infect. Immun.* **58**:1664–1670.
  98. **Zalkin, H.** 1985. NAD synthetase. *Methods Enzymol.* **113**:297–302.
  99. **Zhao, Y., J.-H. Sohn, and J. R. Warner.** 2003. Autoregulation in the biosynthesis of ribosomes. *Mol. Cell. Biol.* **23**:699–707.